Electronic Supplementary Information

Triethanolamine stabilized non-alkyl Sn_4Cd_4 and alkyl Sn_2Cd_{12} oxo clusters with distinct electrocatalytic activities

Di Wang[a, b], Guang-Hui Chen[a], San-Tai Wang[a, b], Jian Zhang[a] and Lei Zhang[a]*

[a] State Key Laboratory of Structural Chemistry, Fujian Institute of Research on the Structure of Matter, Chinese Academy of Sciences, Fuzhou, Fujian, 35002, P. R. China

[b] University of Chinese Academy of Science, 100049, Beijing, P. R. China

* *Corresponding Author*

E-mail: LZhang@fjirsm.ac.cn

Methods

Materials and Instruments. All the chemical reagents were commercially purchased and used without further purification. SnF_2 and butyltin oxide were purchased from Energy Chemical, Cadmium hydroxide was purchased from Aladdin. KCl was purchased from Alfa, while triethanolamine, ethanol, N, N-Dimethylformamide (DMF), acetonitrile and ethylenediamine were bought from Sino pharm Chemical Reagent Beijing. IR spectrum was obtained on a Vertex 7.0 spectrometer with pressed KBr pellets in the range of 4000-400 cm^{-1}. Thermogravimetric analysis was performed on a Mettler Toledo TGA/SDTA 851^e thermal analyzer in flowing N_2 atmosphere with a heating rate of 10 ^oC/min. Powder XRD patterns was obtained by using a Miniflex Ⅱ diffractometer with CuK_α radiation (λ = 1.54056 Å). Elemental analyses (C, H and N) were performed on a vario MICRO elemental analyzer. ICP analysis was conducted by using Inductively Coupled Plasma MS spectrometer (Agilent 7700). (details of sample preparation: a certain amount of bulk samples (**TOC-40**~0.06 g, **TOC-41**~0.06 g) were placed in a digestion tank, then excess aqua regia was added and heated to 200 ^oC until completely digested).X-ray photoelectron spectroscopy (XPS) analysis was carried out on ESCALAB Xi^+ XPS sys tem (Thermo Fisher Scientific) with Al Kα X-ray radiation (1486.6 eV). The 1H NMR experiments were carried on a JNM-ECZ400S spectrometer at frequency of 400 MHz. Gas chromatography (GC) was performed with an GC-2014C (SHIMADZU) gas chromatography system equipped with flame ionization detectors and a thermal conductivity detector (TCD). The liquid products were detected by CIC-D100 automatic range ion chromatograph.

Synthesis of TOC-40. SnF_2 (0.157 g, 1.0 mmol), $Cd(OH)_2$ (0.146 g, 1.0 mmol), triethanolamine (1ml), acetonitrile (4ml) and 1 drop ethylenediamine, 2 drop H_2O were mixed and then sealed in a vial and transferred to a preheated oven heated to 80 ^oC for 4 days. After cooling to room temperature, colorless crystals of **TOC-40** were obtained with a yield of ~32% based on Sn. Elemental analysis (%) for $C_{36}H_{80}Cd_4F_4N_6O_{22}Sn_4$, calc: Sn, 24.36; Cd, 23.06; C, 22.18; H, 4.14; N,4.31. Found: Sn, 23.87; Cd, 22.44; C, 22.27; H, 4.36; N,4.33.

Synthesis of TOC-41. Butyltin oxide (0.05g, 0.24mmol), $Cd(OH)_2$ (0.2 g, 1.36 mmol), KCl (0.01g, 0.13mmol), triethanolamine (1ml), N, N-Dimethylformamide (4ml) and 1 ml ethanol were mixed and then sealed in a vial and transferred to a preheated oven heated to 80 ^oC for 3 days. After cooling to

room temperature, yellow crystals of **TOC-41** were obtained with a yield of ~65% based on Cd. Elemental analysis (%) for $C_{57}H_{114}Cd_{12}Cl_4N_8O_{29}Sn_2$, calc: Sn, 7.65; Cd, 43.46; C, 22.06; H, 3.70; N,3.61. Found: Sn, 9.18; Cd, 43.52; C, 22.94; H, 3.73; N,4.15.

Single-crystal X-ray diffraction. TOC-40 were collected on Hybrid Pixel Array detector equipped with Ga-Kαradiation (λ= 1.3405 Å) at about 99.99 K. **TOC-41** was collected on Supernova single crystal diffractometer equipped with graphite-monochromatic Cu Kα radiation (λ = 1.54178 Å) at 100 K. The program SADABS was used for absorption correction. Structure was solved by direct method and refined by full-matrix least-squares on F^2 using SHELXTL.[1] Non-hydrogen atoms were refined anisotropically. CCDC 2144824-2144825 contain the supplementary crystallographic data for this paper. These data are provided free of charge by The Cambridge Crystallographic Data Centre.

Electrochemical Measurements. Electrochemical experiments were performed on a CHI 760e electrochemical workstation (Chenhua, Shanghai, China) using a gas-tight two-compartment electrochemical cell with a Nafion-117 proton exchange membrane as the separator. Each compartment contained 20 mL of 0.5 M $KHCO_3$ electrolyte, and the electrolyte was pre-saturated with high-purity Ar or CO_2 (Ar: pH = 8.74; CO_2: pH = 7.50). The platinum net (1.0 ×1.0 cm^2) electrode and the Ag/AgCl electrode (the saturated KCl filling solution) were used as counter and reference electrode, respectively. The reference electrode potentials were converted to the value versus RHE by the equation: E (vs. RHE) = E (vs. Ag/AgCl) + 0.197 V + 0.0591 V × pH. The working electrode was prepared by pipetting the 50 uL of sample ink onto a carbon paper electrode (1×1 cm^2) with a loading of 0.53 mg/cm^2. Typically, 5.3 mg of sample was dispersed into H_2O/ethanol (370/80 uL) solution followed by adding 50 uL Nafion, then the mixture was ultrasonicated for 30 min to achieve a homogeneous ink.

For CO_2 electroreduction reaction, a flow of 20 sccm of CO_2 was continuously bubbled into the electrolyte to maintain its saturation. The linear sweep voltammetry (LSV) was performed at a scan rate of 5 mV/s. The electrolysis was conducted at selected potentials for 2 h to determine the reduction products and their Faradaic efficiencies.

Additional details for product analysis of CO_2 electroreduction. Analysis of liquid products by NMR: 10.0 mL of D_2O was mixed with 3.53 μL of dimethyl sulfoxide (DMSO) as solution A for next step. Then, 500 μL of the electrolyte after electrolysis was mixed with 100 μL of D_2O and 50 μL of solution A (DMSO as internal standard) for ^1H NMR analysis. The water suppression method was used.

The gaseous products (H_2 and CO) were periodically sampled and examined by gas chromatography (GC-2014C, SHIMADZU) with N_2 as the carrier gas. They were first analyzed by a thermal conductivity detector (TCD) for the H_2 concentration, and then analyzed by flame ionization detector (FID) with a methanizer for CO. The concentration of gaseous products was quantified by the integral area ratio of the reduction products to standards.

The faradic efficiency of formate was calculated as follow [3]:

$$FE(\%) = \frac{Q_{formate}}{Q_{total}} = \frac{n_{formate} \times N \times F \times 100\ \%}{j \times t} \qquad (1)$$

Where $n_{formate}$ is the measured amount of formate in the cathodic compartment; N is the number of electrons required to form a molecule of formate (N = 2); F is the Faraday constant; j is the recorded current; t is the reaction time.

The faradic efficiencies of gaseous products were calculated as follow [3]:

The volume of the sample loop (V_0) in GC is 1 cm^3 and the flow rate of the gas is v = 20 cm^3/ min. The time it takes to fill the sample loop is:

$$t_0 = \frac{V_0}{v} = \frac{1\ cm^3}{20\ cm^3/min} = 0.05\ min = 3\ s \qquad (2)$$

According to the ideal gas law, under ambient temperature of 25 °C, the amount of gas in each vial (V_0 = 1 cm^3) is:

$$n = \frac{P \times V_0}{R \times T_0} = \frac{1.013 \times 10^5\ Pa \times 1 \times 10^{-6}\ m^3}{8.314\ J \cdot K^{-1} \cdot mol^{-1} \times 298.15\ K} = 4.0866 \times 10^{-5}\ mol \qquad (3)$$

The number of electrons required to form a molecule of CO or H_2 are 2. Therefore, the number of electrons (n_i) needed to get x_i ppm of CO or H_2 is:

$$n_i = x_i \times n \times N_A \times 2 \qquad (4)$$

Total number of electrons (n_{total}) measured during this sampling period:

$$n_{total} = \frac{j \times t_0}{e} \qquad (5)$$

The Faraday constant F is:

$$F = N_A \times e = 6.022 \times 10^{23}\ mol^{-1} \times 1.6022 \times 10^{-19}\ C = 96484.484\ C \cdot mol^{-1} \qquad (6)$$

Hence, the faradic efficiency of CO or H_2 is

$$\mathrm{FE}(\%) = \frac{n_i}{n_{total}} \times 100\ \% = \frac{x_i \times n \times F \times 2}{I_0 \times t_0} \times 100\ \% \qquad (7)$$

Where i represents CO or H_2; I_0 is the recorded current obtained from the chronoamperogram; N_A is the Avogadro constant; e is elementary charge.

References

[1] Sheldrick GM. *SHELXL-2014/7*: A Program for Structure Refinement; University of Göttingen: Göttingen, Germany, (2014).

[2] A. L. Spek, *Acta Cryst*., 2015, **C71**, 9.

[3] D. Ren, Y. L. Deng, A. D. Handoko, C. S. Chen and S. Malkhandi, *ACS Catal*., 2015, **5**, 2814.

Table S1. Crystal data summary for **TOC-40** and **TOC-41.**

Compound	**TOC-40**	**TOC-41**
Cryst. Formula	$C_{36}H_{80}Cd_4F_4N_6O_{22}Sn_4$	$C_{57}H_{114}Cd_{12}Cl_4N_8O_{29}Sn_2$
Fw	1949.42	3013.54
Crystal system	Monoclinic	Tetragonal
space group	$P2_1/n$	$I4_1/acd$
a/ Å	11.8087(9)	25.1808(6)
b/ Å	17.2847(12)	25.1808(6)
c/ Å	14.4581(9)	27.0021(8)
α/deg.	90	90
β/deg	105.059(7)	90
γ/deg	90	90
V/ Å^3	2849.7(4)	17121.3(10)
Z	2	8
Dc /g·cm^{-3}	2.272	2.408
F(000)	1884.0	11904.0
T /K	100.15	100.00(11)
μ /mm^{-1}	17.554	29.697
θ range /°	7.076 to 113. 816	7.02 to 150.53
Reflections collected	19019	17015

Independent reflections	5804	4368
GOF (F^2)	1.019	1.076
R_1/wR_2 [$I > 2\sigma(I)$]	0.0641/ 0.1742	0.0858/ 0.2210
R_1/wR_2[a] (alldata)	0.0858/ 0.1887	0.0899/ 0.2244

[a] $R_1 = \Sigma||F_o|-|F_c||/\Sigma|F_o|$, $wR_2 = [\Sigma w(F_o^2-F_c^2)^2/\Sigma w(F_o^2)]^{1/2}$

Table S2. Selected bond lengths (Å) for **TOC-40**.

Bond	Length(Å)	Bond	Length(Å)
Sn2-O9	2.188(7)	Cd1-O9	2.399(6)
Sn2-O8	2.097(6)	Cd1-O4[1]	2.294(6)
Sn2-O10	2.063(7)	Cd1-O8	2.264(7)
Sn2-N3	2.543(8)	Cd1-O6	2.258(7)
Sn1-F1	1.984(6)	Cd1-N2	2.437(7)
Sn1-O7[1]	2.085(7)	Cd2-O9	2.330(7)
Sn1-O4	2.061(7)	Cd2-O4[1]	2.469(6)
Sn1-F2	1.944(7)	Cd2-O1[1]	2.347(7)
Sn1-O3	2.037(7)	Cd2-O10	2.275(8)
Sn1-O6	2.009(6)	Cd2-O3[1]	2.339(8)
Cd1-O7[1]	2.543(6)	Cd2-N1[1]	2.418(9)
Cd1-O7	2.430(7)	Cd2-O2[1]	2.398(7)

11-X,1-Y,1-Z

Table S3. Selected bond lengths (Å) for **TOC-41**.

Bond	Length(Å)	Bond	Length(Å)
Sn1-O5	2.081(11)	Cd1-O2	2.388(10)
Sn1-O1^{2}	2.091(14)	Cd1-O7	2.489(12)
Sn1-O1	2.091(14)	Cd1-N8	2.388(13)
Sn1-O4	2.102(16)	Cd1A-O5	2.341(9)
Sn1-O4^{2}	2.102(16)	Cd1A^{2}-O5	2.341(9)
Sn1-C1	2.18(3)	Cd2A^{2}-O5	2.263(10)
Cd3-O7	2.208(9)	Cd2A-O5	2.263(10)
Cd3-O3^{1}	2.234(10)	Cd1A^{2}-O7	2.491(13)
Cd3-O6^{1}	2.319(11)	Cd2A-O7	2.069(13)
Cd3-O2^{2}	2.312(10)	Cd1A-O3	2.059(13)
Cd3-Cl1	2.442(4)	Cd2A-O3	2.514(13)
Cd2-O5	2.365(5)	Cd2A-O6	2.504(16)
Cd2-O7	2.323(9)	Cd1A-O1	2.392(15)
Cd2-O3	2.241(9)	Cd2A-N43	2.358(14)
Cd2-O6	2.353(12)	Cd2A-N4	2.359(14)
Cd2-N4	2.369(11)	Cd2A-O8	2.613(14)
Cd2-O8	2.607(10)	Cd2A^{1}-O8	2.613(14)
Cd1-O5	2.327(4)	Cd1A-N8	2.324(14)
Cd1-O3	2.299(9)	Cd2A-O4	2.325(15)

Cd1-O1	2.325(12)	Cd1A-O2	2.418(13)

[1]1-X,3/2-Y,+Z; [2]5/4-Y,5/4-X,5/4-Z; [3]-1/4+Y,1/4+X,5/4-Z

Table S4 BVS calculation of Sn atom in **TOC-40**

Sn2	2.085			Sn1	4.17		
Sn2	O9	d=2.188(7)	0.511	Sn1	F1	d=1.984(6)	0.683
Sn2	O8	d=2.094(7)	0.661	Sn1	O7[1]	d=2.085(7)	0.615
Sn2	O10	d=2.063(7)	0.717	Sn1	O4	d=2.061(7)	0.656
Sn2	N3	d=2.543(8)	0.196	Sn1	F2	d=1.944(7)	0.761
				Sn1	O3	d=2.037(7)	0.700
				Sn1	O6	d=2.009(6)	0.755

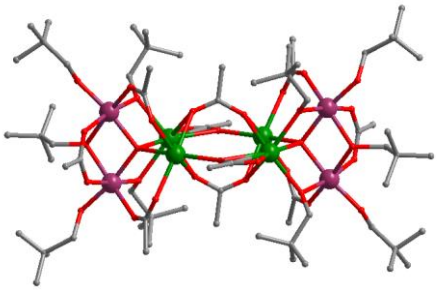

Figure S1. The molecular structure of reported Sn_4Cd_4**.**

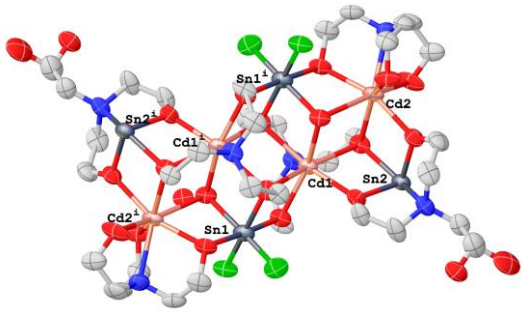

Figure S2. Thermal ellipsoid plots of **TOC-40** presented at the 50% probability level.

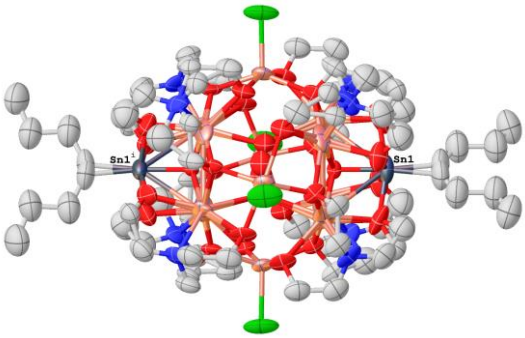

Figure S3. Thermal ellipsoid plots of **TOC-41** presented at the 50% probability level.

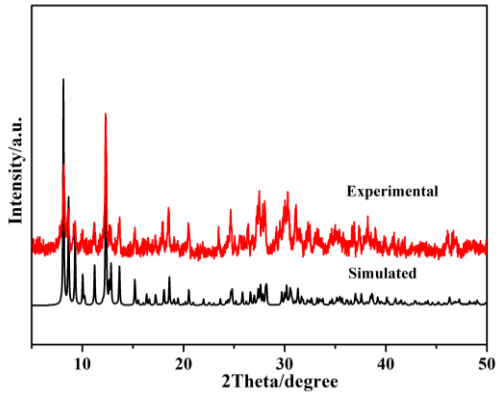

Figure S4. Simulated and experimental PXRD patterns of **TOC-40**.

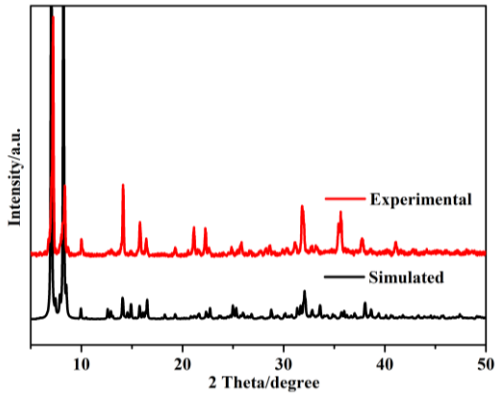

Figure S5. Simulated and experimental PXRD patterns of **TOC-41**.

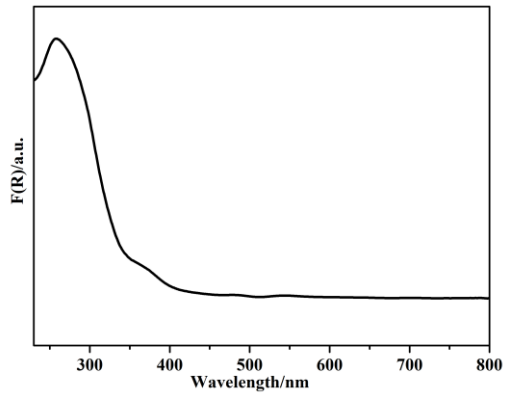

Figure S6. UV-vis diffuse reflectance spectrum of compound **TOC-40**.

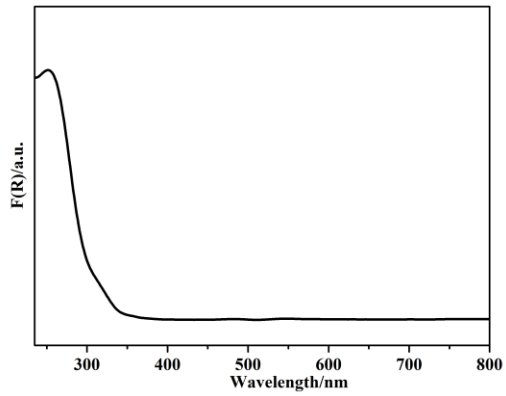

Figure S7. UV-vis diffuse reflectance spectrum of compound **TOC-41**.

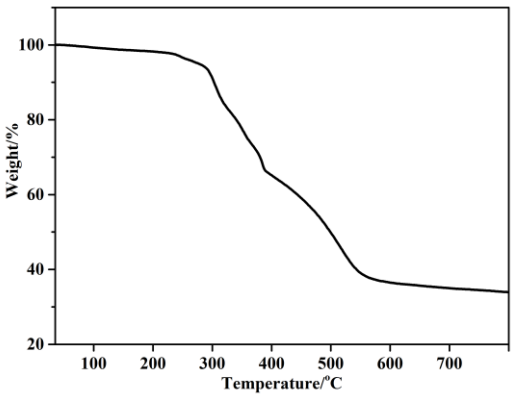

Figure S8. TG curve of compound **TOC-40** in N_2 atmosphere.

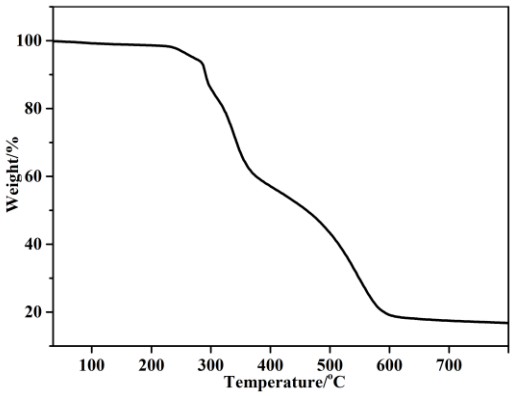

Figure S9. TG curve of compound **TOC-41** in N_2 atmosphere.

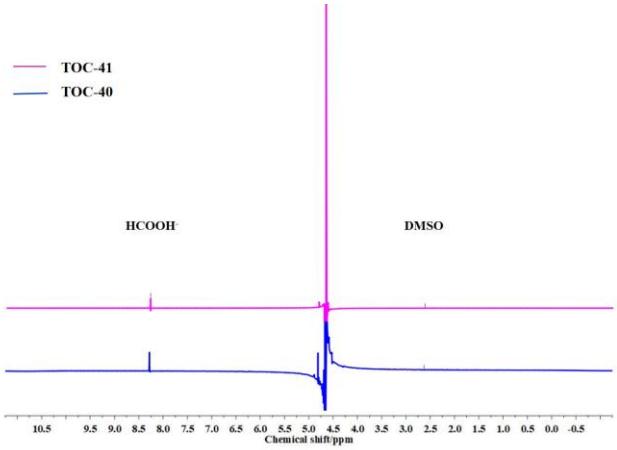

Figure S10. ^{1}H NMR spectrum of the $KHCO_3$ catholyte after 1200 s of CO_2 reduction on **TOC-40**, **TOC-41** derived electrodes, *E*(RHE) = –1.0 V.

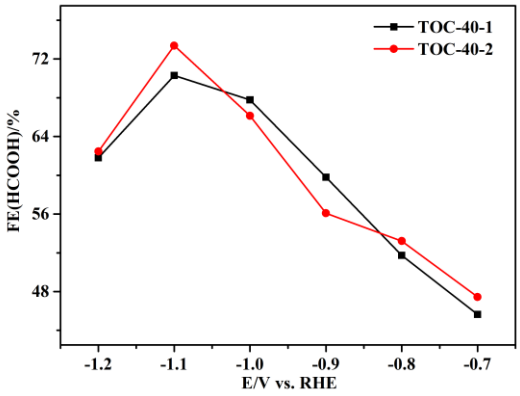

Figure S11. Comparison of formate Faraday efficiency in two electrocatalysis experiments using **TOC-40**.

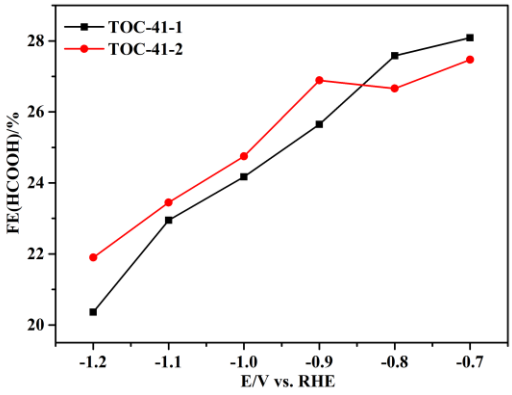

Figure S12. Comparison of formate Faraday efficiency in two electrocatalysis experiments using **TOC-41**.

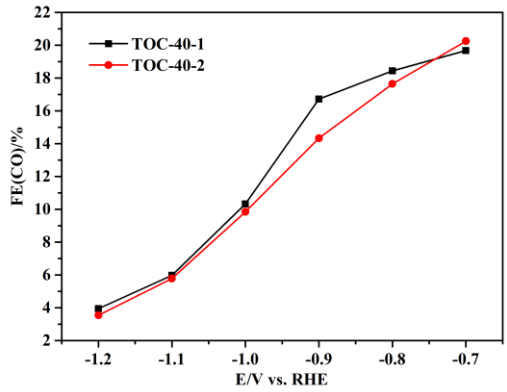

Figure S13. Comparison of CO Faraday efficiency in two electrocatalysis experiments using **TOC-40**.

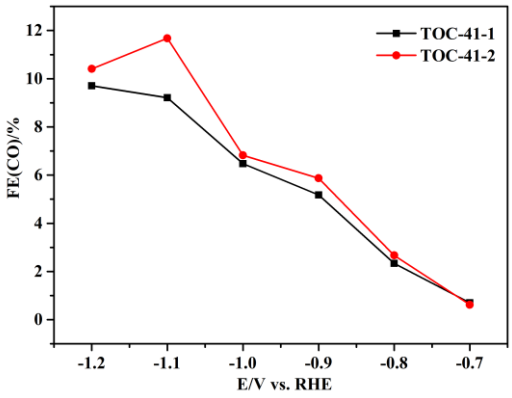

Figure S14. Comparison of CO Faraday efficiency in two electrocatalysis experiments using **TOC-41**.

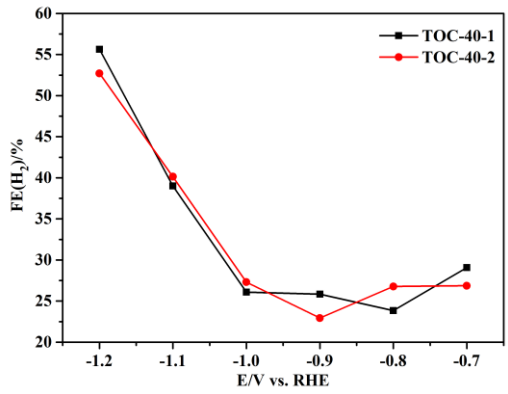

Figure S15. Comparison of H_2 Faraday efficiency in two electrocatalysis experiments using **TOC-40**.

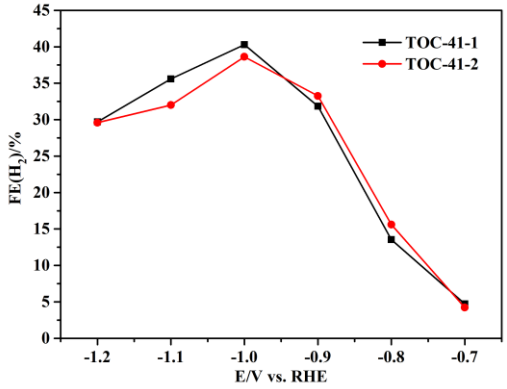

Figure S16. Comparison of H_2 Faraday efficiency in two electrocatalysis experiments using **TOC-41**.

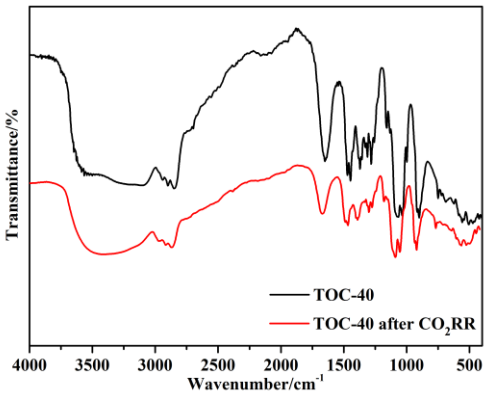

Figure S17. IR spectrum of compound **TOC-40** before and after CO_2RR.

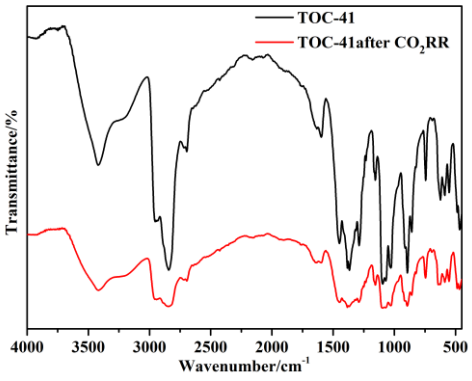

Figure S18. IR spectrum of compound **TOC-41** before and after CO_2RR.